Production of Nanocrystalline RDX by Rapid Expansion of Supercritical Solutions

Victor Stepanov

US Army, RDECOM-ARDEC, Armaments Engineering Technology Center, Picatinny, NJ 07806-5000 (USA)

Lev N. Krasnoperov*, Inga B. Elkina

Department of Chemistry and Environmental Science, New Jersey Institute of Technology, University Heights, Newark, NJ 07102 (USA)

Xuyean Zhang

Material Characterization Laboratory, New Jersey Institute of Technology, University Heights, Newark, NJ 07102 (USA)

Abstract

Nanoscale crystals of cyclotrimethylenetrinitramine (RDX) were produced by Rapid Expansion of Supercritical Solutions (RESS). The experiments were performed by expansion of supercritical solutions of RDX in carbon dioxide through sapphire nozzles (ID: 100 and 150 μm) at pressures of 15.0 – 29.5 MPa and temperatures of 343 – 348 K. Recrystallized particles were characterized by Field Emission Scanning Electron Microscopy (FESEM), X-ray diffraction, HPLC and melting point analysis. The process produced particles with a mean size in the range 110 – 220 nm and a narrow size distribution. The product was crystalline as determined by X-ray diffraction. The effect of process conditions (*T*, *P*, nozzle diameter) on the crystal size distribution was determined.

Keywords: Nanoscale Crystals, RDX, RESS, CO_2, Supercritical Solution

1 Introduction

The development of energetic materials with improved performance yet reduced sensitivity is a major objective in the advancement of high density energetic materials. Explosives belonging to the nitramines family such as RDX, HMX and CL-20 have been studied most extensively due to their high energy density. However, high initiation sensitivity renders these materials dangerous, thus limiting their utilization.

Sensitivity of explosives is related to their chemical as well as physical characteristics. The discovery of new explosives is rare. However, the physical characteristics of an existing explosive can be altered. These include crystal size, shape, morphology, purity, inclusions, internal and external defects, and the microstructure of the intercrystalline voids.

Current theories of the initiation process of explosives are mainly focused on the formation of localized "hot spots" within the explosive upon compression [1]. Hot spots may be formed by adiabatic compression of intercrystalline as well as intracrystalline voids. Other internal defects such as crystal dislocations may also contribute to the formation of hot spots.

Existing theoretical models for the impact initiation of explosives indicate that the sensitivity to external stimuli, such as impact-induced high rate deformation, should decrease with decreasing crystal size [2]. Available experimental data indicate that the sensitivity to stimuli such as impact or shock is decreased as the crystal size is reduced. Gifford et al. investigated the properties of submicron RDX and PETN [3]. Significantly reduced sensitivity to long duration shocks was observed. In addition, novel behavior in deflagration to detonation transition was observed with submicron materials.

A study by Seitz indicates that shock spreading is greatly improved in charges composed of smaller crystals [4]. In a series of experiments utilizing the Floret test, it was observed that the acceptor explosive composed of finer TATB crystals showed a significantly improved detonation spreading as compared to the coarser TATB.

In light of these trends of explosives characteristics with respect to crystal size, it would be of great interest to explore the properties of nanocrystalline energetic materials. However, the majority of traditional micronization techniques, including milling, are not suitable for production of nanoscale particles.

Production of nanoscale crystals involves challenges in the crystallization process as well as in the collection. Very high supersaturation levels are required to achieve nanosized crystals in a crystallization process. Such high supersaturations are unattainable by conventional methods. Collection of nanoparticles is another challenge, due to the difficulties in separation using conventional techniques based on filtration or sedimentation.

In this work, the RESS process was successfully used for the production of nanocrystalline RDX with tunable crystal size down to ca. 100 nm with a narrow size distribution. Particles were characterized by Field Emission Scanning Electron Microscopy (FESEM), X-ray diffraction, HPLC and melting point analysis. Correlations of the parameters of the particles' size distribution with the process conditions were established.

* Corresponding author; e-mail: Krasnoperov@ADM.njit.edu

 DOI: 10.1002/prep.200500002

Crystals formed by the RESS process are anticipated to have high surface quality since the small size is achieved by direct crystallization, without physical grinding, where damage to the crystal surface occurs.

One of the major anticipated benefits is the reduction in the sensitivity to impact initiation. In addition, reactivity of nanocrystalline RDX is anticipated to improve due to a higher ratio of surface to bulk molecules. This ratio becomes substantial in crystals smaller than 100 nm. Quantum chemical calculations indicate that the dissociation of the N-NO_2 bond of the surface molecules requires significantly lower energy than that of the bulk RDX molecules [5].

Prior work by U. Teipel investigated recrystallization of explosives TNT and NTO by RESS using carbon dioxide as a solvent [6]. TNT recrystallization yielded crystals with 10 μm median particle size. Submicron particles of NTO were also reported.

2 The RESS Process

Highly compressed gases are known to dissolve solids (a large body of the solubility data has been compiled elsewhere [7]). Solubilities become significant near the critical point of the solvent and increase with density and temperature. As a result, the solubility can be controlled by manipulation of both temperature and pressure, whereas for liquid solutions only temperature manipulation is available.

The pressure dependence of the solubility offers novel routes in crystallization of dissolved solids. Rapid depressurization of a supercritical solvent brings about drastic changes in the solvent power on a very short time scale. Depressurization to near atmospheric pressure can occur on the timescale of microseconds. This results in high supersaturations, followed by rapid homogeneous nucleation and crystal growth. Supersaturations above 10^6 can be easily achieved with the RESS process [8]. Such drastic solubility changes are not achievable with conventional crystallization techniques.

Basic principles of the RESS process are schematically illustrated in Figure 1. Rapid expansion of a supercritical solution leads to a high supersaturation, the condition at which the critical nucleus size is small. Subsequently, rapid homogeneous nucleation results in a high concentration of small nuclei and leads to the formation of fine, uniform particles. Particles produced by RESS are characteristically ultra-fine (nano- or micrometer range) with a relatively narrow size distribution [9 – 10]. The crystals are expected to be void and defect free. The resulting powders are pure since complete separation from gaseous carbon dioxide is easily achieved.

Crystal size is strongly dependent on the pre-expansion conditions including temperature, pressure, and the solute concentration. In addition, the nozzle geometry can also influence expansion dynamics, affecting the expansion rate and consequently the particle nucleation and growth kinetics.

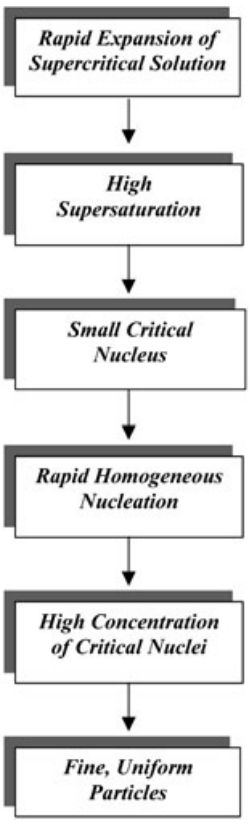

Figure 1. The basic principles of the RESS process.

3 Experimental

3.1 Experimental Setup

Carbon dioxide was chosen as the solvent for RDX recrystallization by RESS. Carbon dioxide has relatively mild critical conditions with $T_c = 304.19$ K and $P_c = 7.382$ MPa [11], low toxicity and environmental impact as well as a low cost. The schematic of the RESS setup is shown in Figure 2. The setup consists of components obtained from Thar Designs Inc. Saturation of supercritical carbon dioxide takes place inside a 1 L heatable high-pressure vessel. For improved saturation, the vessel was packed with 3-mm glass

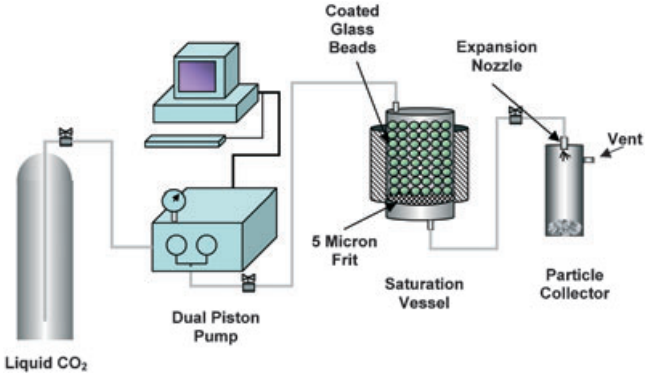

Figure 2. Schematic representation of the RESS setup.

beads coated with RDX. Carbon dioxide was pumped to the saturation vessel with a Thar P-200 dual piston pump capable of maximum CO_2 pumping rate of 200 g/min. The pump piston heads as well as the incoming carbon dioxide were chilled to around 273 K to eliminate formation of vapor CO_2 inside the piston head, which results in a drastic drop in the pumping efficiency. After pumping, the carbon dioxide was heated to the desired temperature prior to being transferred to the saturation vessel.

The saturated RDX/CO_2 solution was transferred through a heated, 1/8" stainless steel tubing to the temperature-controlled nozzle assembly. The tubing was heated to a temperature matching the saturator temperature. A sapphire disk with a laser-drilled orifice was used as a nozzle. The nozzle housing was uniformly heated with imbedded heating elements. The nozzle was situated inside the collection vessel. The vessel was equipped with an exhaust line and a pressure relief valve. Most of the product was collected on the bottom of the collection vessel and some on the internal wall of the vessel. All heating zones and the pump were regulated by the process control software on a local PC.

3.2 Materials

Production grade RDX, which contains about 12% HMX by weight, was used in the experiments. "Bone Dry" grade carbon dioxide was used as the solvent. The solubility of RDX in carbon dioxide has been reported over a temperature range of 303 – 353 K and pressure range of 6.9 – 48.0 MPa [12]. Above 15.0 MPa, the RDX solubility increases with pressure and temperature with a maximum measured solubility of about 0.25 mg of RDX/g of CO_2 at 48.0 MPa and 353 K. Below the critical point the solubility becomes negligible.

3.3 Procedure

RDX coated glass beads, which were used in the saturation vessel, were prepared by spraying and evaporation of RDX/acetone solutions onto pre-heated glass beads. The beads were loaded into the 1 L vessel, and after that the vessel was sealed. The saturation vessel, transfer lines, nozzle assembly and the heat exchangers were heated to the desired operating temperatures. Preheated carbon dioxide was pumped to the vessel until the desired operating pressure was reached. The exit valve was opened establishing flow out of the nozzle. The pumping rate of carbon dioxide was set according to the desired operating pressure.

3.4 Analysis

Recrystallized RDX samples were deposited onto glass slides. Particle size and shape analysis was performed with a Field Emission Scanning Electron Microscope (FESEM LEO 1530 VP) and FESEM software (LEO Electron Microscopy, Inc.). Typically, the variable pressure mode, InLens detector, low voltages, fast scan rate and small aperture were employed for all samples. Before analyzing, the samples were coated with carbon using BAL-TEC MED 020 HR Sputtering Coater. Image-Pro Plus software (MediaCybernetics) was used for image analysis, particle size measurements and size distribution calculations. Thermal properties were analyzed with a Perkin Elmer Diamond DT/TGA. X-ray powder diffraction analysis was performed with a Scintag 2000 diffractometer. Chemical composition was analyzed by Waters 2695 HPLC.

4 Results and Discussion

The effects of the pre-expansion conditions (temperature, pressure, and the nozzle diameter) on the RDX particle size were investigated. Both temperature and pressure strongly influence the solubility of RDX in supercritical carbon dioxide as well as the expansion dynamics. The solution flow rate is dictated by the nozzle orifice diameter for a given pressure.

One series of experiments was performed keeping the pre-expansion temperature constant at 343 ± 5 K. The pre-expansion pressure was in the range 15.0 – 29.5 MPa, varied

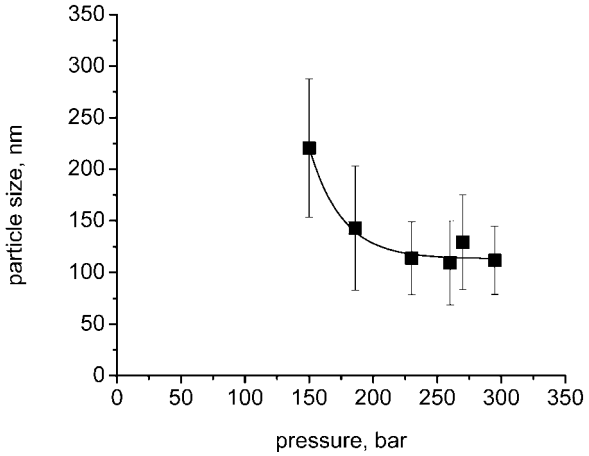

Figure 3. Effect of the pre-expansion pressure on the RDX particle size at 343 K.

Table 1. Experimental conditions and the corresponding size of recrystallized RDX particles, produced by the RESS process.

Pre-expansion conditions		Nozzle ID	RDX particle size
T/K	$P/10^5$ Pa	μm	nm
344	150	100	220 ± 70
341	186	100	140 ± 60
338	230	100	110 ± 35
343	260	100	110 ± 40
341	270	100	130 ± 45
348	295	100	110 ± 30
348	280	100	125 ± 40
363	150	100	115 ± 35
363	150	150	140 ± 30

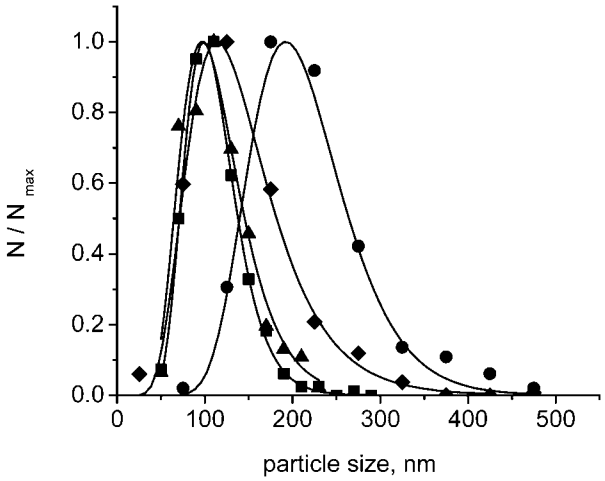

Figure 4. Lognormal size distribution functions (solid lines) and experimental data (symbols) for RDX particles produced at 343 K and different pressures: 15.0 (●), 18.6 (◆), 23.0 (▲) and 29.5 MPa (■); N_{max} is the number of particles per bin in the maximum, N is the number of particles in a bin.

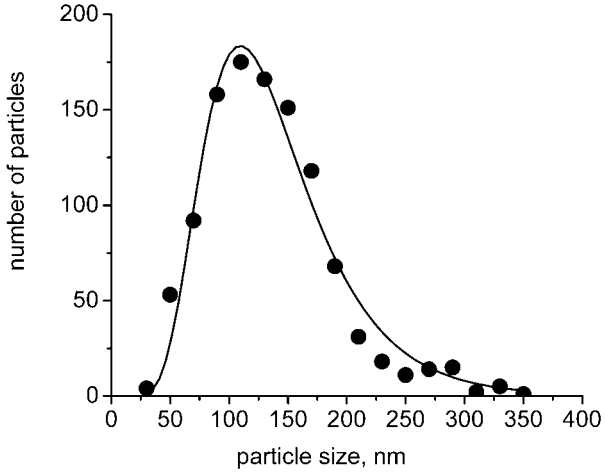

Figure 6. Lognormal size distribution function (solid line) and experimental data (symbols) of RDX particles produced at 348 K and 28.0 MPa. The particle size is 125 ± 40 nm.

by carbon dioxide flow rate. The orifice diameter was 100 μm. Figure 3 illustrates the effect of pre-expansion pressure on the mean particle size at 343 K. (The mean particle size is defined by Image-Pro Plus software, as an average of the diameters measured at 2 degree intervals.) The results are also listed in Table 1. At the highest pressure studied, RDX crystals with a particle size of 110 ± 30 nm were produced. At the lowest pressure, particles with a size of 220 ± 70 nm were obtained. Figure 4 shows the particle size distribution of four samples, taken at 343 ± 5 K and different pre-expansion pressures. The particle size distributions are best fitted by the lognormal distribution function. Increasing pressure leads to a decrease in the particle size. However, at higher pressures (23.0 – 29.5 MPa) this dependence becomes weaker (Figure 3).

Qualitatively, this result is in accordance with the classical nucleation theory. The solubility of RDX in CO_2 increases with pressure. Higher concentrations result in higher supersaturations upon expansion. As the supersaturation increases, the critical nucleus size decreases and the nucleation rate increases. This leads to high concentration of critical nuclei and to small final particle size.

In a series of runs to produce approximately 1 g of nanocrystalline RDX, the conditions were set to 348 K and 28.0 MPa. The solubility of RDX at these conditions is 0.11 mg of RDX/g of CO_2 [12]. A SEM image and the particle size distribution of a sample taken from the final product are respectively illustrated in Figures 5 and 6.

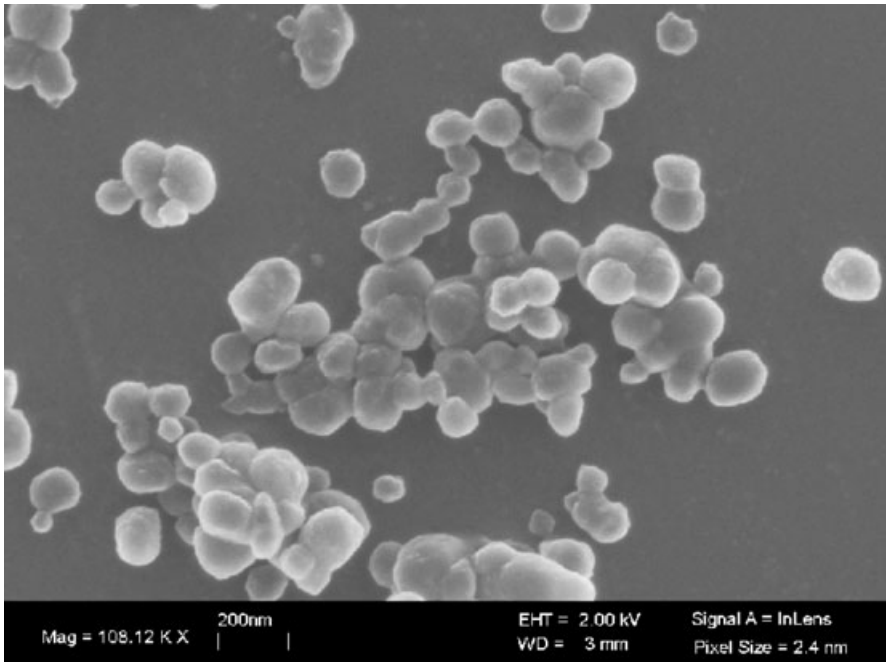

Figure 5. Sample SEM image of RDX particles produced at 348 K and 28.0 MPa.

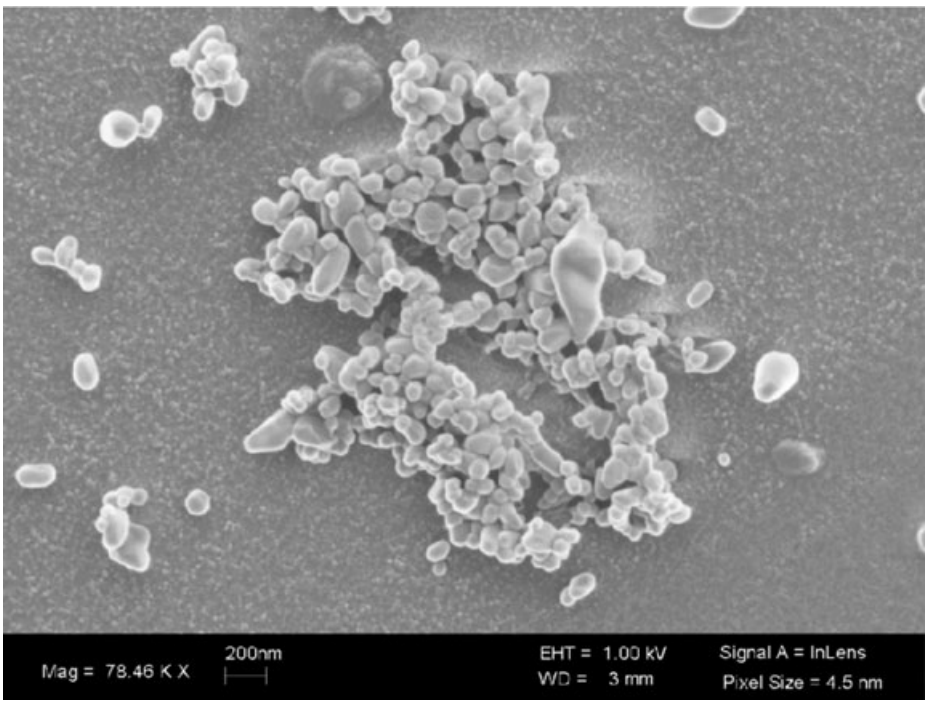

Figure 7. Sample SEM image of RDX particles produced at 363 K and pressure 15.0 MPa using heatable nozzle (ID = 100 μm). The particle size is 115 ± 35 nm.

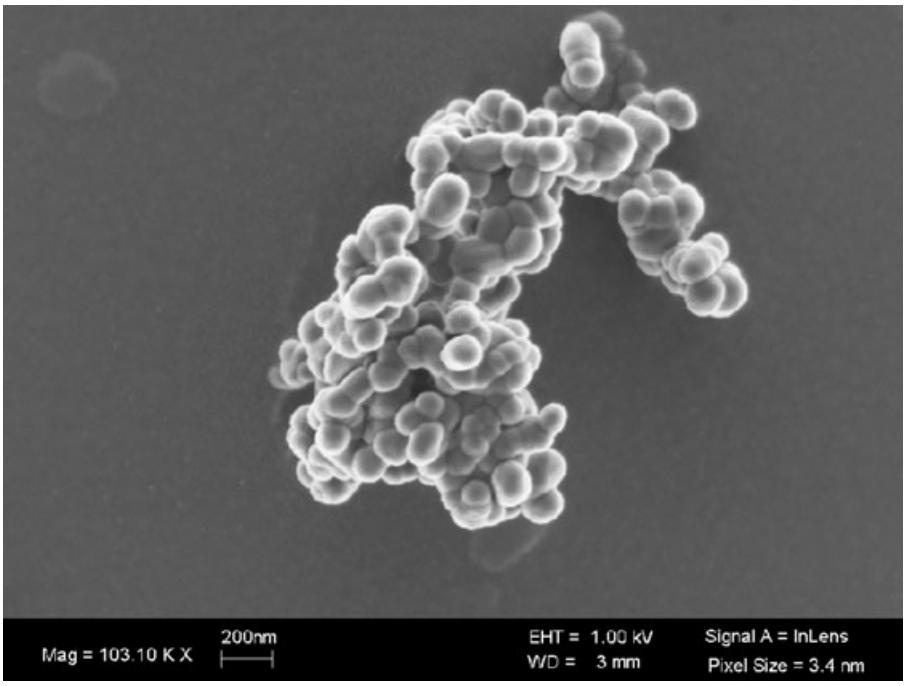

Figure 8. Sample SEM image of RDX nano-particles produced at 363 K and pressure 15.0 MPa using heatable nozzle (ID = 150 μm). The particle size is 140 ± 30 nm.

Additional experiments were performed with a 150 μm orifice. Figures 7 and 8 depict the SEM images of particles formed at 15.0 MPa and 363 K, using 100 and 150 μm ID nozzles, respectively. At the conditions examined, smaller RDX particles were produced using a smaller, 100 μm orifice (Table 1).

4.1 Properties of Nanocrystalline RDX

The particles produced in all experiments have a round or oval shape. X-ray powder diffraction was used to determine whether the particles are crystalline or amorphous. Figure 9 illustrates the X-ray diffraction data for the recrystallized and the precursor RDX. Peak intensity (arbitrary units) is

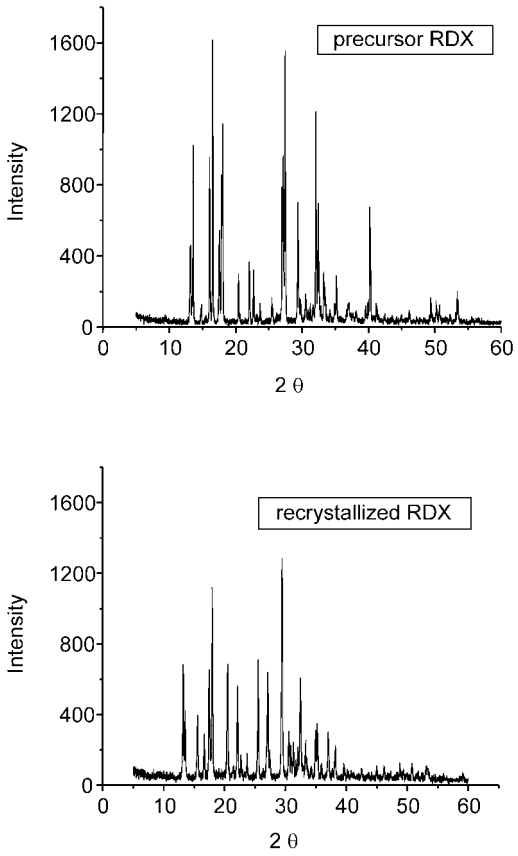

Figure 9. X-ray diffraction spectra for the precursor RDX and recrystallized RDX.

plotted as a function of the diffraction angle (2θ). Narrow peaks are indicative of crystalline structure.

HPLC analysis was used to determine the chemical composition. The precursor RDX contains 12% HMX by weight. The HMX content in the recrystallized RDX was less than 1%. This result reveals the strong solubility difference of RDX and HMX in supercritical CO_2 and is in accordance with the published supercritical carbon dioxide extraction data of RDX and HMX [13, 14].

The melting point analysis was performed using a Perkin Elmer Diamond DT/TGA. The melting point of pure RDX was 477 K. The melting point of the recrystallized RDX was 476 K.

5 Conclusion

The RESS process, utilizing carbon dioxide as solvent, was successfully implemented in the production of nanocrystalline RDX. The capability to finely tune the particle size in the range 110 – 220 nm with a narrow size distribution was experimentally demonstrated. The effects of the key process parameters on the particle size were determined. Characterization of the product indicates crystalline structure and a melting point similar to that of the convention pure RDX.

6 References

[1] P. J. Miller, C. S. Coffey and V. F. DeVost, Heating in Crystalline Solids due to Rapid Deformation, *J. Appl. Phys.* **1986**, *59*, 913.
[2] R. W. Armstrong, C. S. Coffey, V. F. DeVost and W. L. Elban, Crystal Size Dependence for Impact Initiation of Cyclotrimethylenetrinitramine Explosive, *J. Appl. Phys.* **1990**, *88*, 979.
[3] M. J. Gifford, A. Chakravarty, M. Greenaway, S. Watson, W. Proud and J. Field, Unconventional Properties of Ultrafine Energetic Materials, *32nd Int. Annual Conference of ICT*, Karlsruhe, Germany, July 3 – 6, **2001,** p. 100.
[4] W. L. Seitz, Short-Duration Shock Initiation of Triaminotrinitribenzene (TATB), *Proceedings of the American Physical Society*, Topical Conference, Santa Fe, NM, 18 – 21 July **1983**, p. 531.
[5] M. M. Kuklja, Chemical Decomposition of Solid Cyclotrimethylene Trinitramine, *2001 International Conference on Computational Nanoscience and Nanotechnology*, Hilton Oceanfront Resort, South Carolina, USA, 19 – 21 March, **2001**, Vol. 2, 73.
[6] U. Teipel, Production of Particles of Explosives, *Propellants, Explos., Pyrotech.* **1999**, *24*, 134.
[7] K. D. Bartle, G. F. Shilstone, S. A. Jafar and A. A. Clifford, Solubilities of Solids and Liquids of Low Volatility in Supercritical Carbon Dioxide, *J. Phys. Chem. Ref. Data.* **1991**, *20*, 713.
[8] P. G. Debenedetti, Homogeneous Nucleation in Supercritical Fluids, *AIChE J.* **1990**, *36*, 1289.
[9] J. W. Tom and P. G. Debenedetti, Particle Formation with Supercritical Fluids - A Review, *Aerosol Sci.* **1991**, *22*, 555.
[10] M. Turk, Formation of Small Organic Particles by RESS: Experimental and Theoretical Investigations, *J. Supercrit. Fluids* **1999**, *15*, 79.
[11] C. L. Yaws, *Chemical Properties Handbook*, McGraw-Hill, New York, **1998**, 784.
[12] J. B. Morris, Solubility of RDX in Dense Carbon Dioxide at Temperatures between 303 K and 353 K, *J. Chem. Eng. Data.* **1998**, *43*, 269.
[13] P. G. Thorne, *Evaluation of the Use of Supercritical Fluids for the Extraction of Explosives and Their Degradation Products from Soil*, CRREL Special Report 94 – 9, **1994**, US Army Corps of Engineers, Hanover, NH.
[14] W. H. Griest, C. Guzman and M. Dekker, Packed-column Supercritical Fluid Chromatographic Separation of Highly Explosive Compounds, *J. Chromatography A*. **1989**, *467*, 423.

Acknowledgements

This work was supported by US Army ARDEC under contract number DAAE30 – 02-C-1140 and was funded by the Picatinny Arsenal Nanovalley program. The authors are grateful to Mr. Steven M. Nicolich and Dr. Reddy Damavarapu for valuable advice and helpful discussions.

(Received June 24, 2004; Ms 2004/116)

